Inorganic Chemistry Communications 12 (2009) 1094–1098

Contents lists available at ScienceDirect

Inorganic Chemistry Communications

journal homepage: www.elsevier.com/locate/inoche

Organometallic ruthenium complexes with thiosemicarbazone ligands: Synthesis, structure and cytotoxicity of $[(\eta^6\text{-}p\text{-cymene})Ru(NS)Cl]^+$ (NS = 9-anthraldehyde thiosemicarbazones)

Floyd A. Beckford [a,*], Gabriel Leblanc [a], Jeffrey Thessing [a], Michael Shaloski Jr. [a], Brian J. Frost [b], Liya Li [c], Navindra P. Seeram [c]

[a] Science Division, Lyon College, Batesville, AR 72501, USA
[b] Department of Chemistry, University of Nevada, Reno, NV 89557, USA
[c] Department of Biomedical and Pharmaceutical Sciences, College of Pharmacy, University of Rhode Island, Kingston, RI 02881, USA

ARTICLE INFO

Article history:
Received 29 June 2009
Accepted 29 August 2009
Available online 4 September 2009

Keywords:
Thiosemicarbazones
Ruthenium–arene complex
DNA interaction
Viscometry
Cytotoxicity
Structure elucidation

ABSTRACT

A series of half-sandwich arene ruthenium complexes containing bidentate thiosemicarbazone ligands have been synthesized and their biological activity investigated. The compounds have the general formula [(6-*p*-cymene)Ru(R-ATSC)Cl]X (ATSC = 9-anthraldehyde thiosemicarbazone and R = H, CH_3 and C_6H_5). The crystal structure of [(6-*p*-cymene) Ru(MeATSC)Cl]Cl have been determined and represents the first structurally characterized arene–ruthenium half-sandwich complex with a thiosemicarbazone ligand. The complexes show good cytotoxic profiles against MCF-7 and MDA-MB-231 (breast adenocarcinoma) as well as HCT 116 and HT-29 (colorectal carcinoma) cell lines.

Introduction. Thiosemicarbazones are of considerable pharmacological interest since a number of derivatives have shown a broad spectrum of chemotherapeutic properties. The wide range of biological activities possessed by substituted thiosemicarbazones and their metal complexes include cytotoxic, antitumor, antibacterial and antiviral properties. This is particularly true for the heterocyclic thiosemicarbazones [1]. It has been suggested that the antitumor activity of heterocyclic thiosemicarbazones is due to the compounds modifying the reductive conversion of ribonucleotides to deoxyribonucleotides as a result of the inhibition of the ribonucleotide reductase enzyme which inhibits DNA synthesis [2]. The ligands coordinate to metal ions inside the cell, forming complexes which supposedly act as the true active species. The biological properties of the ligands can be modified and in fact enhanced, by the linkage to metal ions [3,4].

Metal complexes are used in many fields of drug discovery. Platinum coordination compounds are widely used as antitumor drugs. The first platinum antitumor drug introduced in the clinic were *cis*-diamminedichloroplatinum(II) (cisplatin) and it has become the most widely used anticancer drug in the world. The clinical efficacy of cisplatin and other platinum drugs is diminished by intrinsic and acquired tumor resistance. In addition cisplatin has high toxicity, leading to side effects which limit the administered dose [5]. These limiting issues has led to an intense effort to design new transition metal-based compounds that are capable of overcoming problems associated with cisplatin while maintaining the same level of activity and broadening the spectrum of the therapeutic effect. In attempts to find a new, metal-based anticancer drug with activity complementary to cisplatin, several ruthenium complexes have recently been investigated for their antitumor activity. Very recently, two ruthenium-(III) complexes have also successfully completed phase I clinical trials, namely, NAMI-A [6–8] {NAMI-A, (ImH)[*trans*-Ru(III)-Cl_4Im(Me_2SO)]; Im – imidazole}, and KP1019 indazolium *trans*-[tetrachlorobis(1*H*-indazole)ruthenate(III)] [9,10].

Organometallic half-sandwich ruthenium(II)–arene complexes are currently attracting increasing interest as anticancer compounds. Recently, developed ruthenium(II) complexes of the type $[(\eta^6\text{-arene})Ru(en)Cl][PF_6]$ (en = ethylenediamine) show promising anticancer activity [11]. These monofunctional Ru(II) arene complexes have been considered novel antitumor agents with a mechanism of action different from that of NAMI-A or KP1019. While DNA binding is believed to be the mechanism of action, other factors such as cell uptake will affect the cytotoxic activity and is dependent on the nature, particularly the size, of the arene [11,12]. In addition, they were found to be active toward cisplatin-resistant cells [13,14].

* Corresponding author. Tel.: +1 870 307 7212; fax: +1 870 307 7496.
E-mail address: floyd.beckford@lyon.edu (F.A. Beckford).

1387-7003/$ - see front matter © 2009 Elsevier B.V. All rights reserved.
doi:10.1016/j.inoche.2009.08.034

In this paper, we report on a study (synthesis, characterization and cytotoxicity) of a series of half-sandwich organometallic ruthenium complexes containing thiosemicarbazones as the chelating ligand.

Results and discussion. *Syntheses and characterization:* Complex **1** was synthesized in 54% yield by refluxing $[(\eta^6\text{-}p\text{-cymene})RuCl_2]_2$ [15] with the ligand [16] in a 2:1 mole ratio in methanol followed by addition of NH_4PF_6. The solid was recrystallized from CH_2Cl_2 and ether (Scheme 1). Complexes **2** and **3** were synthesized by reacting $[(\eta^6\text{-}p\text{-cymene})RuCl_2]_2$ with the ligand in CH_2Cl_2 at room temperature, concentrating the reaction solution and adding ether to precipitate the product (Scheme 1). The reaction produced red or orange solids that are insoluble in alcohols and water but are very soluble in acetone, CH_2Cl_2 and DMSO. For complex **2**, crystals suitable for structure determination were grown by slow diffusion of ether into a CH_2Cl_2 solution of the complex.

NMR spectral studies: The NMR spectra of the complexes were run in DMSO-d_6 as they are very soluble in this solvent. Similar to other *p*-cymene complexes, **1** and **3** show a loss of the twofold symmetry of the *p*-cymene ligand [17] upon coordination of the thiosemicarbazone ligand. This is evidenced by four sets of doublets for the aromatic hydrogen on the *p*-cymene ligand found between 6.27–6.52 ppm for **1** and 5.95–6.02 ppm for **3** [18]. Additionally in **3**, the methyl groups of the isopropyl moiety are inequivalent, observed as two singlets at 1.17 and 1.27 ppm. The aromatic protons of the thiosemicarbazone ligand show up between 7.57 and 8.50 ppm, similar to the free ligands. The hydrazinic proton shifts slightly on binding and the imine (HC=N) proton shifts downfield by as much as 0.15 ppm upon coordination.

Infrared spectra: Thiosemicarbazones exhibit characteristic bands corresponding to various groups in specific energy regions. The most significant IR bands in the region 4000–500 cm^{-1} are found between 3150–3450 (assigned to NH stretching vibrations); 1580–1625 (assigned to C=N + NH); and ~820–900 (assigned to C=S vibration). The characteristic absorption peaks of all complexes are similar. There are three or two bands in the ν(N–H) region and these signals play an important role in evaluating the nature of the bonding in thiosemicarbazone complexes. The presence of a band corresponding to hydrazinic N(2)–H group, suggests the coordination of a thiosemicarbazone to the metal center in a neutral form, while its absence, is suggestive of deprotonation in the complexes. In all the complexes, there is a band at ~3200–3130 cm^{-1} which is assigned to the hydrazinic N(2)–H group and this support the thione formulation of the ligand in the complexes. The other band(s) (at ~3450–3350 cm^{-1}) are the stretching vibrations of the terminal amino N(3)–H group and do not shift significantly on complexation; the shift is due to change in the electron density upon complexation of the thiocarbonyl sulfur. In the complexes the medium intensity band ascribed to ν(C=N) are shifted by up to 25 cm^{-1} to lower energy upon complexation. This negative shift indicates that the azomethine nitrogen (N(1)) coordinates to the metal [19,20]. The involvement of the thiocarbonyl group can similarly be inferred from the wavenumber shifts that occur on binding. The band in the free ligand at ~840 cm^{-1} which we attribute to the C=S group shifts to lower frequencies by 5–25 cm^{-1}. The size of the shifts suggest that the ligand coordinates as a neutral, bidentate (through the azomethine nitrogen and thiocarbonyl sulfur) ligand in all the complexes.

Crystal structure: Crystallographic data for **2**·CH_2Cl_2 are given in Table 1. This represents the first example of a structurally characterized half-sandwich ruthenium arene complex with a thiosemicarbazone ligand. The molecular structure of cation **2** (Fig. 1) adopts the archetypical piano-stool geometry of ruthenium half-sandwich arene complexes. The metal is coordinated by the *p*-cymene, a terminal chloride and the chelating thiosemicarbazone ligand. The relevant bond lengths and selected bond angles are given in Table 2. The metal center has essentially octahedral coordination geometry with some distortion. The RuCl, RuS and RuN are comparable to other structurally characterized ruthenium are complexes with similar N–S donor ligands (unpublished work). Hamaker [21] have reported a series of complexes with an imine–thioether donor set, $[(\eta^6\text{-}p\text{-cymene})RuCl(MeSC_6H_4\text{-}2\text{-}N{=}CH{-}C_6H_4\text{-}p\text{-}X]^+$; these complexes have RuN bond lengths ranging from 2.099–2.132 Å, RuCl bond lengths from 2.3978 to 2.4227 Å and RuS from 2.3397 to 2.3496 Å. Our values of 2.1452(6) Å, 2.4169(17) Å and 2.3547(6) Å are only slightly longer. The bond angles through ruthenium involving the three legs of the piano-stool are in the range of 82–86° indicating a distortion from a regular octahedron (90°). The average RuC_{arene} bond of 2.215 Å is in line with other ruthenium arene half-sandwich complexes [22] and the Ru–centroid distance is 1.699 Å which is similar to our unpublished compounds and close to the values reported by the Hamaker group. The *p*-cymene ligand is somewhat asymmetrically coordinated to the ruthenium. The Ru(1)–C(6) and Ru(1)–C(7) bonds (average 2.258 Å) are somewhat longer than the Ru(1)–C(8) and Ru(1)–C(9) pair (average 2.175 Å). Among the other pair, Ru(1)–C(4) and Ru(1)–C(5 have different lengths. All this leads to a twist in the arene ligand at C(4), possibly to limit any steric interaction between C(1) methyl of the isopropyl group and the S(1) of the thiosemicarbazone ligand.

Electrochemistry: The electrochemical (cyclic voltammetry) behavior of the complexes has been studied in dichloromethane using a scan rate of 100 mV/s and tetrabutylammonium hexafluorophosphate as the supporting electrolyte. The complexes showed similar features in the investigated sweep range (0–2.0 V). There is one irreversible oxidation wave (Fig. 2) corresponding to the Ru(II)/Ru(III) couple: relative to the Fc/Fc^+, E_{pa} was 1024, 1042, 1106 mV for complexes **1**, **2** and **3,** respectively. There is also

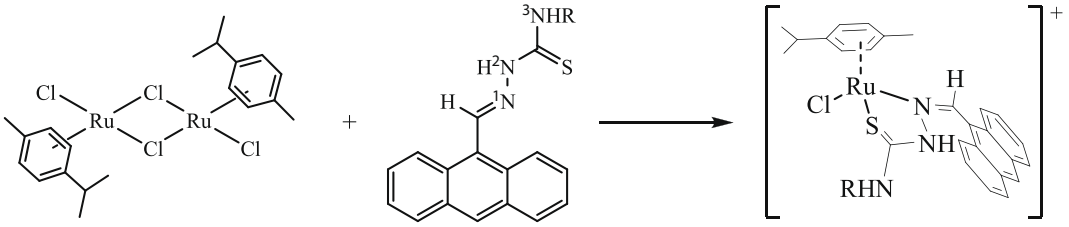

thiosemicarbazone = N-S

R = H (**1**): (i) 2 N-S, CH_3OH, Δ, 90 min (ii) NH_4PF_6
R = CH_3 (**2**) and R = C_6H_5 (**3**): (i) 2 N-S, CH_2Cl_2, RT, 2-4h (ii) Ether

Scheme 1. Synthesis of $[(\eta^6\text{-}p\text{-cymene})Ru(R\text{-}ATSC)Cl]X$; X = Cl^-, PF_6^-.

Table 1
Selected crystallographic and refinement data for **2**·CH_2Cl_2.

Parameter	Value
Empirical formula	$C_{28}H_{31}Cl_4N_3SRu$
Formula weight	684.49
T (K)	100(2) K
Wavelength (Å)	0.71073 Å
Crystal system	Triclinic
Space group	$P\bar{1}$
a (Å)	10.492(2)
b (Å)	11.546(2)
c (Å)	12.835(3)
α (°)	82.230(5)
β (°)	76.541(5)
γ (°)	77.429(5)
Volume (Å^3)	1470.0(5)
Z	2
D_{calc} (Mg/m^3)	1.546
Absorption coefficient (mm^{-1})	0.991
Crystal size (mm^3)	0.37 × 0.26 × 0.05
θ Range	1.64–26.00
Index ranges	$-12 \leqslant h \leqslant 12$, $-14 \leqslant k \leqslant 12$, $-15 \leqslant l \leqslant 12$
No. reflections collected	23,578
No. independent reflections	5727 [R_{int} = 0.0221]
Absorption correction	SADABS
Data/rest./param.	5727/0/334
GOF F^2	1.059
Final R indices; [$I > 2\sigma(I)$]	R_1 = 0.0252; wR_2 = 0.0679
R indices (all data)	R_1 = 0.0269; wR_2 = 0.0688

an ill-defined oxidation wave at higher potential (near 1700 mV) that becomes more defined as the scan rate increased. As far as we know there are no reports of electrochemical studies on half-sandwich ruthenium arene complexes with thiosemicarbazones.

Table 2
Selected bond lengths [Å] and angles [°] for **2**·CH_2Cl_2.

Ru(1)–C(4)	2.218(2)	Ru(1) –Cl(1)	2.4169(6)
Ru(1) –C(5)	2.205(2)	Ru(1) –N(1)	2.1453(17)
Ru(1) –C(6)	2.259(2)	Ru(1) –S(1)	2.3547(6)
Ru(1) –C(7)	2.257(2)	N(1) –Ru(1) –S(1)	81.83(5)
Ru(1) –C(8)	2.179(2)	N(1) –Ru(1) –Cl(1)	81.66(5)
Ru(1) –C(9)	2.170(2)	S(1) –Ru(1) –Cl(1)	86.37(2)

So another comparison with the Hamaker [21] complexes (E_{pa} 1180–1336), suggest that with the thione as opposed to the thioether group, the ruthenium center is more easily oxidized.

Interaction of complexes with ct-DNA: In biological systems, complexes will encounter an array of biomolecules with which they could potentially react. Hence, it is important to gain a detailed understanding of such interactions. Since DNA is the primary target of the classical platinum anticancer drugs, binding studies of ruthenium(II) arene complexes with this molecule is important. It is recognized that the nature of the arene group affects the mode of binding of these complexes to DNA. It has been reported that for a series of complexes, [(η^6-arene)Ru(en)(Cl)]$^+$ intercalation or groove binding is the principal mode of interaction when the arene is biphenyl or anthracene derivatives, group that possess flat extended aromatic rings [23]. The mode was different for the *p*-cymene derivative. In order to investigate the interaction mode between the complexes and ct-DNA, the ethidium bromide (EB) fluorescence displacement experiment was also employed. EB emits intense fluorescent light in the presence of DNA due to its strong intercalation between the adjacent DNA base pairs. The displacement technique is based on the decrease of this fluorescence resulting from the displacement of EB from a DNA sequence by a

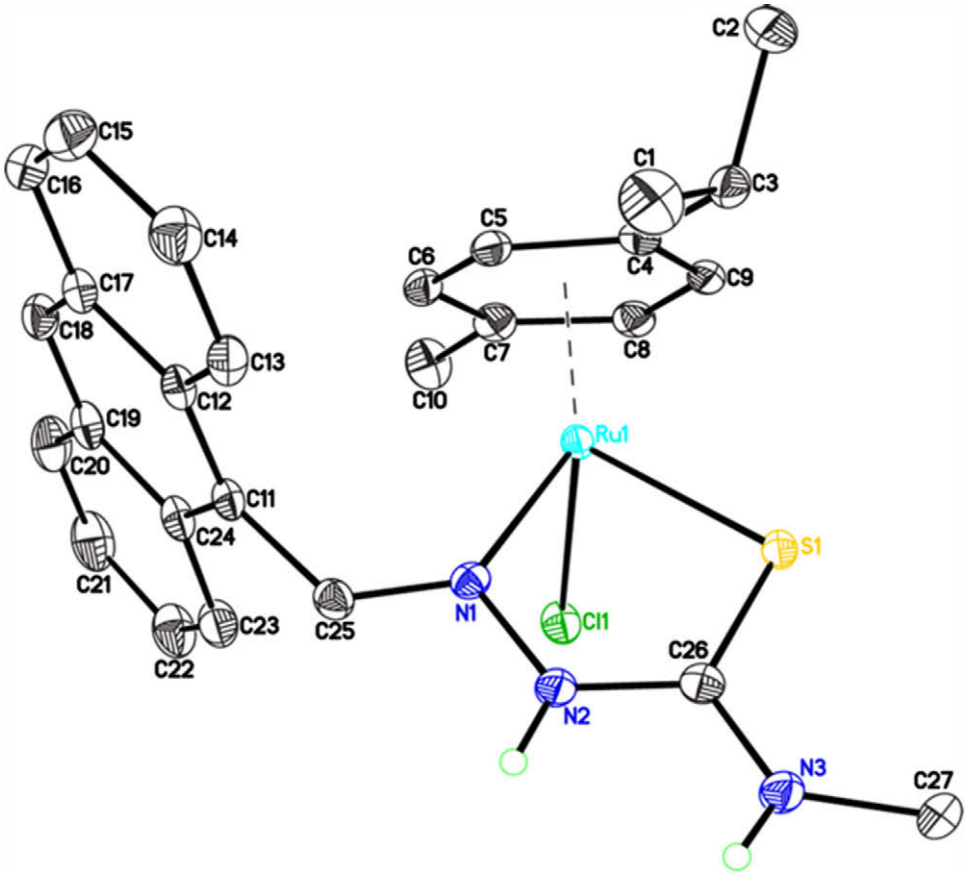

Fig. 1. Molecular structure of complex **1** with hydrogen atoms omitted for clarity.

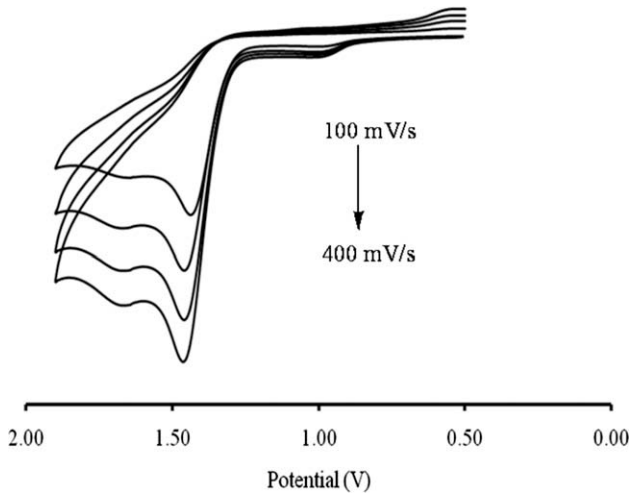

Fig. 2. Cyclic voltammograms for **1** (1×10^{-3} M) measured in CH_2Cl_2 (vs. Ag/AgCl) at various scan rates.

quencher. The quenching is due to the reduction of the number of binding sites on the DNA that is available to the EB. The method therefore provides indirect evidence for an intercalative binding mode. The extent of fluorescence quenching may also be used to determine the extent of binding between the quencher and DNA. Complex **1** was used to illustrate this concept. On titration of the EB-DNA solution with **1**, there is reduction in the fluorescence intensity at λ_{em} = 600 nm as the [Ru] increases. The spectra show no significant changes in shape or wavelength. This clearly indicates that some EB molecules are displaced from their DNA binding sites and replaced by the complex and it is fair to conclude that some intercalation has occurred. A quantitative estimation of quenching can be obtained from a Stern–Volmer analysis of the data. According to the Stern–Volmer Eq. (1) [24], the relative fluorescence is directly proportional to the concentration of the quencher:

$$\frac{F_0}{F} = 1 + K_{SV}[Q] \quad (1)$$

where F_0 and F are the fluorescence emission intensities of the EB-DNA system before and after the addition of the complexes, K_{SV} is the Stern–Volmer quenching constant and [Q] is the concentration of the quencher (1). The quenching constants, calculated from the slope of the Stern-Volmer plot (F_0/F vs. [Q]) shown in Fig. 3, were found to be $3.73 \times 10^3\ M^{-1}$ and $2.17 \times 10^3\ M^{-1}$ at 298 K and 303 K, respectively. The linearity of the quenching plots illustrate that the quenching is in good agreement with the Stern–Volmer equation. The linearity also indicates that only one type of quenching process is in operation. It is well known that quenching occurs through a static (involving the formation of quencher–fluorophore complex) or dynamic process. High temperatures tend to disrupt ground state complex formation. This fact can be used to establish which mechanism is in operation. The value of the Stern–Volmer quenching constant should decrease with an increase in temperature as the ground state complex becomes less stable. The reverse will be observed for dynamic quenching. The values obtained illustrates that quenching by the complex is predominantly static. A bimolecular quenching constant (K_q) can be calculated from the Stern–Volmer constant: $K_{SV} = K_q\tau_0$, where τ_0 is the lifetime of the fluorophore and is 22 ns [25]. For **1** K_q is at least an order of magnitude larger than the limiting value of $10^{10}\ M^{-1}\ s^{-1}$ [24], considered the largest possible value in aqueous medium. This confirms that the fluorescence quenching is not the result of dynamic quenching, but rather a consequence of static quenching.

Viscometric studies: As a means for further clarifying the binding of the complexes with DNA, the viscosity of DNA solutions containing varying amount of added complex were measured. Photophysical probes such as absorption or fluorescence measurements generally provide significant but inconclusive evidence to support an intercalative binding model. Among the common methods, hydrodynamic methods (viscometry in particular) that are sensitive to DNA length changes are the most definitive tests of the classical intercalation model of binding in solution. Besides the ability to unwind DNA, a classical intercalator will cause an increase in the viscosity of a DNA solution since the DNA helix must lengthen as base pairs are separated to accommodate the binding ligand [26]. According to theory of Cohen and Eisenberg [27] viscosity data were plotted as $(\eta/\eta_0)^{1/3}$ vs. the binding ratio ([Ru]/[DNA]) as shown in Fig. 4. For all the complexes, it was observed that increasing the complex concentration led to a general increase in the viscosity of the DNA solution. Thus together with the results from the EB displacement experiments, we may conclude that the complexes are intercalators. A look at the structure for **2** shows that the *p*-cymene moiety is incapable of intercalation into DNA as the isopropyl subgroup deviates significantly out of the plane. In addition the π-electrons are used in bonding to ruthenium. So it is clear that the flat aromatic portion of the thiosemicarbazone ligand is responsible for the intercalation.

Cytotoxicity studies: Compounds **1–3** were evaluated for their cytotoxicity in a panel of human tumor cell lines – MCF-7 and MDA-MB-231 (breast adenocarcinoma) as well as HCT 116 and HT-29 (colorectal carcinoma) – by means of a colorimetric assay

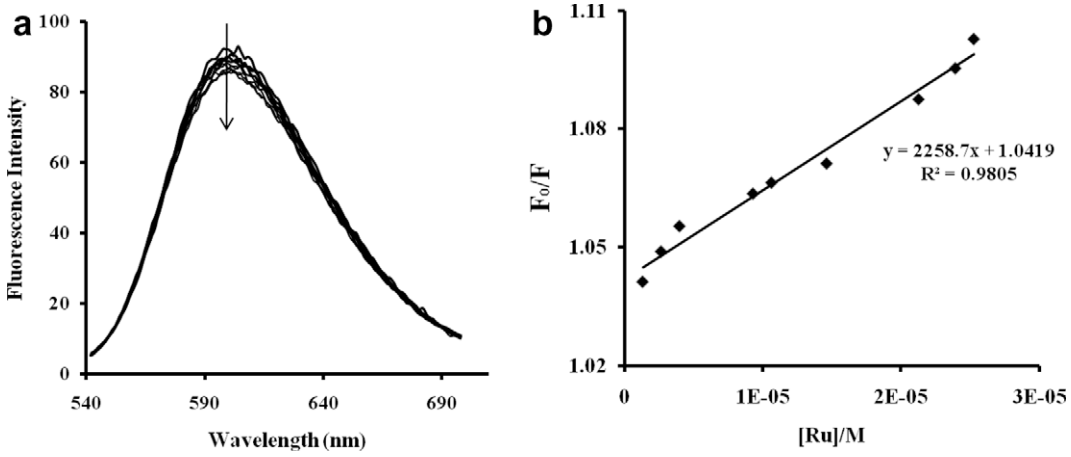

Fig. 3. (a) Fluorescence quenching curves and (b) Stern–Volmer plot of the ct-DNA-bound ethidium bromide with **1** at 303 K.

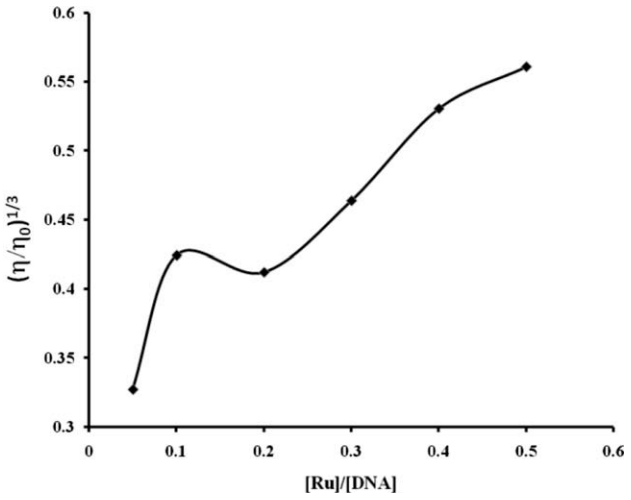

Fig. 4. Effect of the increasing amount of **1** on the relative viscosity of ct-DNA at 306 (±0.1) K; [DNA] = 0.1 mM.

Table 3
Antiproliferative activity of complexes **1**–**3** in panel of four human cancer cell lines.

Compound	IC_{50} (μM)[a]			
	MDA-MB-231	MCF-7	HCT 116	HT-29
1	5.04 ± 0.99	39.2 ± 8.1	9.34 ± 1.08	8.32 ± 3.08
2	2.67 ± 0.38	13.2 ± 0.25	3.27 ± 0.40	4.94 ± 0.50
3	9.01 ± 3.52	18.05 ± 11.8	12.3 ± 0.06	17.4 ± 6.39
Cisplatin	730	506 ± 86	3.10	24.3

[a] 50% inhibitory concentration after exposure for 72 h in the MTS assay. Values are means ± standard deviations.

(MTS assay) which measures mitochondrial dehydrogenase activity as an indication of cell viability. The effects of the compounds on the viability of these cells were evaluated after an exposure period of 72 h. All the complexes showed moderate cytotoxic potencies and their IC_{50} values, corresponding to inhibition of cancer cell growth at the 50% level, are listed in Table 3. As a general observation, complex **2** is the most active against all the cell lines. Also the alkyl group on N(3) is non-innocent as there appears to be an decrease in potency as the alkyl group gets bigger. Between cell lines there is also another clearly discernible trend in that the compounds showed higher activities against the MDA-MB-231 cells, which are estrogen receptor negative (ER(-)) vs. the ER(+) MCF-7 cells. There is a similar trend present in the colon cell lines – activity is higher in the HCT-116 cells which normally does not express cyclooxygenase COX-2.

Acknowledgements

The project described was supported by NIH Grant No. P20 RR-16460 from the IDeA Networks of Biomedical Research Excellence (INBRE) Program of the National Center of Research Resources.

Appendix A. Supplementary material

CCDC 733807 contains the supplementary crystallographic data for this paper. These data can be obtained free of charge from The Cambridge Crystallographic Data Centre via www.ccdc.cam.ac.uk/data_request/cif. Supplementary data associated with this article can be found, in the online version, at doi:10.1016/j.inoche.2009.08.034.

References

[1] D.L. Klayman, J.P. Scovill, J.F. Bartosevich, J. Bruce, J. Med. Chem. 26 (1983) 39.
[2] D. Kovala-Demertzi, M.A. Demertzis, J.R. Miller, C. Papadopoulou, C. Dodorou, G. Filousis, J. Inorg. Biochem. 86 (2001) 555.
[3] J. Garcia-Tojal, A. Garcia-Orad, J.L. Serra, J.L. Pizarro, L. Lezamma, M.I. Arriortua, T. Rojo, J. Inorg. Biochem. 75 (1999) 45.
[4] D.H. Petering, Bioinorg. Chem. 1 (1972) 255.
[5] (a) G. Chu, J. Biol. Chem. 269 (1994) 787–790;
(b) M.A. Fuertes, C. Alonso, J.M. Perez, Chem. Rev. 103 (2003) 645–662;
(c) R. Agarwal, S.B. Kaye, Nat. Rev. Cancer 3 (2003) 502–516.
[6] G. Sava, A. Bergamo, Int. J. Oncol. 17 (2000) 353–365.
[7] J.M. Rademaker-Lakhai, D. Van den Bongard, D. Pluim, J.H. Beijnen, J.H. Schellens, Clin. Cancer Res. 10 (2004) 3717–3727.
[8] (a) G. Sava, R. Gagliardi, A. Bergamo, E. Alessio, G. Mestroni, Anticancer Res. 19 (1999) 969–972;
(b) A. Bergamo, B. Gava, E. Alessio, G. Mestroni, B. Serli, M. Cocchieto, S. Zorzet, G. Sava, Int. J. Oncol. 21 (2002) 1331–1338;
(c) M. Groessl, E. Reisner, C.G. Hartinger, R. Eichinger, O. Semenova, A.R. Timerbaev, M.A. Jakupec, V.B. Arion, B.K. Keppler, J. Med. Chem. 50 (2007) 2185–2193.
[9] (a) C.G. Hartinger, S. Zorbas-Seifried, M.A. Jakupec, B. Kynast, H. Zorbas, B.K. Keppler, J. Inorg. Biochem. 100 (2006) 894–904;
(b) S. Kapitza, M. Pongratz, M.A. Jakupec, P. Heffeter, W. Berger, L. Lackinger, B.K. Keppler, B. Marian, J. Cancer Res. Clin. Oncol. 131 (2005) 101–110;
(c) B.K. Keppler, M. Henn, U.M. Juhl, M.R. Berger, R. Niebl, F.E. Wagner, Prog. Clin. Biochem. Med. 10 (1989) 41–69;
(d) M. Pongratz, P. Schluga, M.A. Jakupec, V.B. Arion, C.G. Hartinger, G. Allmaier, B.K. Keppler, J. Anal. At. Spectrom. 19 (2004) 46–51.
[10] E.D. Kreuser, B.K. Keppler, W.E. Berdel, A. Piest, E. Thiel, Semin. Oncol. 19 (1992) 73–81.
[11] R.E. Morris, R.E. Aird, P. Murdoch del, S.H. Chen, J. Cummings, N.D. Hughes, S. Parsons, A. Parkin, G. Boyd, D.I. Jodrell, P.J. Sadler, J. Med. Chem. 44 (2001) 3616–3621.
[12] O. Novakova, J. Kasparkova, V. Bursova, C. Hofr, M. Vojtiskova, H. Chen, P.J. Sadler, V. Brabec, Chem. Biol. 12 (2005) 121–129.
[13] R.E. Aird, J. Cummings, A.A. Ritchie, M. Muir, R.E. Morris, H. Chen, P.J. Sadler, D.I. Jodrell, Br. J. Cancer 86 (2002) 1652–1657.
[14] S.M. Guichard, R. Else, E. Reid, B. Zeitlin, R. Aird, M. Muir, M. Dodds, H. Fiebig, P.J. Sadler, D.I. Jodrell, Biochem. Pharmacol. 71 (2006) 408–415.
[15] M.A. Bennett, A.K. Smith, Dalton Trans. (1974) 233.
[16] F.A. Beckford, A. Holt, J. Undergraduate Chem. Res. 6 (2007) 173. Briefly, equimolar amounts of 9-anthraldehyde and the appropriate N4 alkyl-substituted thiosemicarbazide were suspended in anhydrous ethanol containing a few drops of glacial acetic acid. The reaction mixture was heated at reflux for 3½ h and after cooling the light precipitate that formed was collected by filtration and washed thoroughly with ethanol followed by ether and dried in the vacuum.
[17] I. Moldes, E. de la Encarnación, J. Roo, Á. Alvarez-Larena, J.F. Pinella, J. Organomet. Chem. 566 (1998) 165.
[18] C.G. Hamaker, D.P. Halbach, J. Organomet. Chem. 691 (2006) 3349.
[19] H. Beraldo, W.F. Nacif, L.R. Teixeria, J.S. Reboucas, Transition Met. Chem. 27 (2002) 85.
[20] D.X. West, J.K. Swearigen, J. Valdee-Martinez, S. Hernandez-Ortegs, A.K. El-Sawaf, F. van Meurs, A. Castineiras, I. Garcia, E. Bermejo, Polyhedron 18 (1999) 2919.
[21] C.G. Hamaker, D.P. Halbach, Polyhedron 28 (2009) 2228.
[22] F.A. Allen, Acta Crystallogr. Sect. B 58 (2002) 380.
[23] O. Novakova, H. Chen, O. Vrana, A. Rodger, P.J. Sadler, V. Brabec, Biochemistry 42 (2003) 11544.
[24] J.R. Lacowicz, Principles of Fluorescence Spectroscopy, 3rd ed., Springer, New York, 2006.
[25] K.S. Ghosh, B.K. Sahoo, D. Jana, S. Dasgupta, J. Inorg. Biochem. 102 (2008) 1711.
[26] E.C. Long, J.K. Barton, Acc. Chem. Res. 23 (1990) 271–273.
[27] G. Cohen, H. Eisenberg, Biopolymers 8 (1969) 45–55.